Connexin26 and 43 play a role in regulating pro-inflammatory events in the epidermis

García-Vega, Laura; O'Shaughnessy, Erin M.; Jan, Afnan; Bartholomew, Christopher; Martin, Patricia E.

Published in:
Journal of Cellular Physiology

DOI:
10.1002/jcp.28206

Publication date:
2019

Document Version
Author accepted manuscript

Connexin26 and 43 play a role in regulating pro-inflammatory events in the epidermis

Laura García-Vega, Erin M. O'Shaughnessy, Afnan Jan, Chris Bartholomew and *Patricia E. Martin.

Department of Life Sciences, School of Health and Life Sciences, Glasgow Caledonian University, Glasgow, G4 0BA, Scotland

*Corresponding author:

Patricia E. Martin. Department of Life Sciences, School of Health and Life Sciences, Glasgow Caledonian University, Glasgow, G4 0BA, Scotland, U.K.

Email: patricia.martin@gcu.ac.uk ; Tel: +44 141 331 3726

ORQUID ID: 0000-0003-0809-8059

Abbreviations: ATP: adenosine triphosphate; CBX: carbenoxolone; Cx: Connexin; h: hour; IL: interleukin; KD: knockdown; KID: keratitis ichthyosis deafness; LPS: lipopolysaccharide; min: minute; Panx: Pannexin; PGN: peptidoglycan; Sf: serum free; TLR2: Toll like receptor 2.

Abstract

Dysregulation of Connexin (Cx) expression and function is associated with a range of chronic inflammatory conditions including psoriasis and non-healing wounds. To mimic a pro-inflammatory environment, HaCaT cells, a model human keratinocyte cell line, were challenged with 10 µg/mL peptidoglycan (PGN) isolated from *Staphylococcus aureus* for 15 minutes to 24 hours in the presence or absence of connexin blockers and/or following *CX26*, *CX43*, *PANX1* and *TLR2* siRNA knock-down (KD). Expression levels of IL-6, IL-8, CX26, CX43, PANX1, TLR2 and Ki67 were assessed by RT-qPCR, western blot and/or immunocytochemistry. NF-kβ was blocked with BAY11-7082, CX-channel function was determined by ATP release assays. ELISA monitored IL6 release following PGN challenge in the presence or absence of siRNA or blockers of connexin or purinergic signalling. Exposure to PGN induced *IL-6*, *IL-8*, *CX26* and *TLR2* gene expression but it did not influence *CX43*, *PANX1* or *Ki67* mRNA expression levels. CX43 protein levels were reduced following 24 h PGN exposure. PGN-induced *CX26* and *IL-6* expression were also aborted by *TLR2*-KD and inhibition of NF-kβ. ATP and IL-6 release were stimulated following 15 min and 1-24 h challenge with PGN respectively. Release of both agents was inhibited by co-incubation with Cx-channel blockers, *CX26*-, *CX43*- and *TLR2*-KD. The IL-6 response was also reduced by purinergic blockers. CX-signalling plays a role in the innate immune response in the epidermis. PGN is detected by TLR2, which via NF-kβ, directly activates *CX26* and *IL-6* expression. CX43 and CX26 maintain pro-inflammatory signalling by permitting ATP release, however PANX1 does not participate.

Keywords: Connexin 26, Connexin 43, Pannexin 1, Peptidoglycan, Toll-Like-Repector2, NF-kB, purinergic signalling, epidermis, inflammation, intercellular signalling.

1. INTRODUCTION

The skin forms a physical barrier between the organism and the external environment, protecting from physical, chemical or biological aggression (Baroni et al., 2012). The epidermis, the outer layer of the skin, is principally composed of keratinocytes that are subclassified into four layers: the basal, spinous, granular and cornified layers. From the basal layer keratinocytes proliferate and differentiate moving throughout the layers until the cornified layer. The epidermis is avascular so the delivery and co-ordination of intercellular signals directly between the cell layers is believed to be directed via gap junction intercellular channels (Martin et al., 2014). Connexins (Cx), the structural building blocks of gap junctions, are a family of 21 different proteins in humans. Up to ten connexins are differentially expressed throughout the stratified epidermis, suggesting a key role in differentiation and maintenance of epidermal integrity (Di et al., 2001). Six connexins oligomerise to form a hemichannel, that is trafficked in a closed state, to the plasma membrane where it aligns and docks with a hemichannel from a neighbouring cell to form a gap junction intercellular channel permitting the interchange of small molecules (<1.2kDa) (Laird, 2006). Under conditions of cell stress connexin hemichannels within the membrane can be induced to open rendering the cell susceptible to release of ATP 'danger- signals' with subsequent effects on downstream purinergic signalling pathways (Ceelen et al., 2011). Two predominant connexins in human epidermis CX43 (encoded by the α gene family member, GJA1) and CX26 (encoded by the β gene family member GJB2) are unable to form heteromeric channels and have distinctive permeability properties, suggesting specialised spatial communication compartments exist within the epidermis (Chanson et al., 2018; Kam et al., 1986). Pannexins (Panx) share structural but not amino acid sequence homology with connexins and also form channels releasing ATP and other signalling molecules into the extracellular milieu. Three isoforms have been identified and two of them are expressed in the skin (Panx3 and mainly PANX1) (Celetti et al., 2010).

Several congenital skin disorders characterised by abnormal keratinisation and hypertrophy are associated with dominant mutations in β-connexin genes and they fall into two main classes (Martin and van Steensel, 2015). Firstly, those with loss of channel function and defective trafficking such as CX26-D66H, associated with Vohwinkel syndrome (OMIM#124500), a hyperproliferative but non-inflammatory skin disorder. Secondly, those CX26 mutations linked with inflammatory disorders such as keratitis ichthyosis deafness syndrome (KID) (OMIM#148210) which is proposed to be caused by 'leaky' hemichannels and is characterised

by the susceptibility of patients to severe bacterial and fungal skin infections (Garcia et al., 2016; Martin and van Steensel, 2015). Recent reports also suggest that these mutations in CX26 alter CX26:CX43 compatibility giving rise to differential signalling properties (Shuja et al., 2016). Deregulation of CX26 and CX43 are also associated with other inflammatory and hyperproliferative skin conditions including chronic non-healing wounds (Brandner et al., 2004; Sutcliffe et al., 2015) and psoriasis, where increased CX26 expression is a hallmark of the condition (Labarthe et al., 1998; Li et al., 2014; Lucke et al., 1999). In addition, psoriatic plaques present a dysbiosis from commensal colonisation (e.g. *Staphylococcus epidermis*) to opportunistic colonisation (e.g. *S. aureus*) (Holland et al., 2009; Sanford and Gallo, 2013), suggesting that a microbiome shift and altered innate immune signalling patterns may contribute to the pathogenesis.

Previously, we determined that peptidoglycan (PGN), a key component of the Gram-positive bacterial cell wall and potent inducer of the innate immune response, triggered ATP release from cells expressing KID mutations but not 'non-KID' mutations (Donnelly et al., 2012). This event subsequently triggered downstream signalling responses, enhancing release of Interleukin 6 (IL-6) that could be reduced by connexin-channel blockers. PGN also modified connexin expression and function in astrocytes, glial and endothelial cells (Ceelen et al., 2011; Esen et al., 2007; Retamal et al., 2007b). Toll-Like receptor 2 (TLR2) is a key receptor associated with triggering innate immune signalling cascades and a variety of studies have reported links between connexin-hemichannel activity and TLR2 signalling events (Ey et al., 2009; Martin and Prince, 2008; Robertson et al., 2010).

In the present work we have explored the impact of PGN on connexin and pannexin expression and function in HaCaT cells, a model keratinocyte cell line that can differentiate and stratify in a manner similar to normal epidermis (Boukamp et al., 1988). We report that PGN induces CX26, TLR2 and IL-6 expression and siRNA-knockdown (KD) strategies indicate that both IL-6 and CX26 are targets of TLR2 activation. Furthermore, CX43 and CX26 expression are linked with activation of connexin-hemichannel activity and induction of the innate immune response, highlighting the potential of connexin-related therapeutic strategies to help regulate inflammatory skin disorders.

2. MATERIALS AND METHODS

2.1. Cell culture

The human keratinocyte cell line HaCaT (Cell Line Service (Boukamp et al., 1988) was maintained in Dulbecco's Modified Eagle's Medium high glucose (4.5 g/L) without L-glutamine (DMEM, SLS, Newhouse, UK) supplemented with 10 % (v/v) Foetal Bovine Serum (FBS, Lonza), 50 U/mL penicillin/streptomycin (SLS, Newhouse, UK) and 2 mM L-glutamine (SLS, Newhouse, UK) (cDMEM). Cells were cultured in a 37 ºC humidified incubator in an atmosphere of 5 % CO2. Under these conditions, HaCaT cells do not stratify but maintain a phenotype similar to that of epidermal basal keratinocytes. Cells were seeded at appropriate densities into 24-well plates for ATP assay (approximately $7.5x10^4$ cells per well), onto 16 mm^2 glass coverslips in a 12-well plate for immunostaining (approximately $1x10^5$ cells per well) and into 6-well plates for ELISA, protein and RNA extraction (approximately $0.5x10^6$ cells per well).

2.2. SiRNA Knock-down

Cells were transfected with appropriate siRNA duplex sequences targeted to *CX26, CX43, TLR2* or *PANX1* (5 nM) (TriFECTa®RNAi Kit, IDT, Leuven, Belgium) or a fluorescently labelled scrambled siRNA transfection control duplex: TYE 563™ (IDT, Leuven, Belgium), using Lipofectamine 3000 according to the manufacturer's instructions (Invitrogen, Paisley, UK). All assays were performed 24 hours (h) post-transfection.

2.3. Cell treatments and challenges

HaCaT cells were treated with serum free medium without antibiotics and supplemented with L-glutamine (sfDMEM) in the presence or absence of the connexin channel blockers 50 µM carbenoxolone (CBX, Sigma Aldrich, Irvine, UK), Gap26 100nM or Gap27 100nM (Zealand Pharma, Glostrup, Denmark) (Faniku et al., 2018; Wright et al., 2009) for 1 h prior to challenge with 10 µg/mL PGN isolated from *S. aureus* (Sigma-Aldrich, Irvine, UK) for 15 minutes (min), 1, 3, 6 or 24 h as described previously (Donnelly et al., 2012). Connexins blockers were in the medium throughout the PGN challenge. HaCaT cells were exposed also to BAY11-7082 (Invivogen, Toulouse, France), an inhibitor of NF-kB, at 10 µM for 24 h (Jiang et al. 2017), suramin (Tocris, Abingdon, UK), an antagonist of P2Y receptors, at 100 µM for 1h (Lee et al. 2001) and A438079 (Tocris, Abingdon, UK), an antagonist of P2X7, at 5 µM for 1h (Mankus et al. 2011) in sfDMEM.

2.4. Reverse-transcription and real-time PCR

RNA was isolated using Nucleospin RNA 11Kit (Bioline, London, UK), DNAse treatment with Ambion DNA-free™ kit (Thermofisher, Paisley, UK) and cDNA synthesised with the M-MLV reverse transcription kit (Promega, Southampton, UK). Taqman real time PCR quantified the expression of *CX26*, *CX43*, *GAPDH*, *PANX1*, *Ki67*, *IL*-6 and *IL-8* (Primer Design, Southampton, UK, and Sigma-Aldrich, Irvine, Scotland, proprietary validated). The PCR mixture contained 1 x Precision PLUS RT-qPCR MasterMix (Primer Design, Southampton, UK), 0.4 µM of each primer and probe, 0.25 ng/µL cDNA and RNase free H_2O adjusted to a final volume to 10 µL. RT-qPCR was performed in a ViiA™ 7 Real-Time PCR System (Thermo Fisher, Paisley, UK) under the following cycling conditions: 95 °C for 15 min, followed by 40 cycles of 95 °C for 15 seconds (s) and 60 °C for 30 s. mRNA levels were obtained from the value of threshold cycle (Ct) for each specific gene and normalised against the Ct of GAPDH (ΔΔCt method (Livak, 2001). Gene fold changes ≥±2 were considered biologically significant (Dalman, 2012).

2.5. Western blot analysis and immunohistochemistry

Cells were harvested in 100 µl ice-cold RIPA lysis buffer (Santa Cruz, Heidelberg, Germany) per well. Total protein (50-100 µg depending on the protein) was separated on 10-12 % (w/v) SDS polyacrylamide gels and transferred to a nitrocellulose membrane (GE Healthcare Ltd, Amersham, UK) using a TE22 Mighty Small Transfer Tank (Hoefer, Holliston, USA) for 3 h at 100 V. Membranes were blocked with 5 % (w/v) skimmed milk in TBS-T (200 mM Tris, 1.5 mM NaCl, 0.1 % (v/v) Tween 20) and probed with primary antibodies: Rabbit polyclonal anti-CX26 1:100 (51-2800, Invitrogen, Paisley, UK), Rabbit polyclonal anti-CX43 1:1000 (Ab-367, Sigma-Aldrich, Irvine, UK), Rabbit polyclonal anti-PANX1 1:1000 (HPA016930, Sigma-Aldrich, Irvine, UK) or Mouse monoclonal anti-GAPDH 1:1000 (sc-32233, Santa Cruz, Heidelberg, Germany) respectively, at 4°C overnight. Secondary antibodies IRDye® 800CW Goat anti-Rabbit IgG (H + L) and IRDye® 680RD Goat anti-Mouse IgG diluted 1:10,000 (LI-COR, Cambridge, UK) were used. The fluorescence was visualised by digital imaging using an Odyssey FC Dual Mode Imaging system (LI-COR, Cambridge, UK) and densitometry values were obtained using Image Studio software. Band densities were normalised to GAPDH protein density values (Taylor et al., 2013).

For immunohistochemistry cells were fixed in ice-cold methanol for 3 min at -20 ˚C, permeabilised by incubation with phosphate-buffered saline (PBS, SLS, Newhouse, UK) and 0.1 % (v/v) Triton X-100 for 30 min at room temperature and blocked with 5 % (w/v) milk-PBS for 30 min. The incubation with the primary antibody was overnight at 4 ˚C, Rabbit

polyclonal anti-CX43 diluted 1:100 (Leithe and Rivedal, 2004), Mouse monoclonal anti-CX26 diluted 1:50 (13-8100, Invitrogen, Paisley, UK) and anti-PANX1 diluted 1:100 (HPA016930, Sigma-Aldrich, Irvine, UK). The secondary antibody was Goat anti-rabbit conjugated to Alexa594 or Alexa488 or Goat anti-mouse conjugated to Alexa488 or Alexa594 (Sigma-Aldrich, Irvine, UK). Nuclei were stained with DAPI (2.5 µg/mL) (Sigma-Aldrich, Irvine, UK). Slides were viewed on a Zeiss LSM 800 confocal microscope (Carl Zeiss Microscopy GmbH, Jena, Germany) enabling visualisation of Alexa488, Alexa594 and DAPI staining. Protein expression levels were semi-quantified by calculating the mean fold change in pixel intensity of treated versus control cells using Zen 2. Blue edition software (Carl Zeiss Microscopy GmbH, Jena, Germany).

2.6. Hemichannel activity assessment: ATP release assay

In experiments where connexin inhibitors were employed, cells were pre-incubated with them for 1 h. Cells were then stimulated with 10 µg/ml PGN or calcium-free PBS (SLS, Newhouse, UK) for 15 min. Following stimulation, 25 µL of each sample was transferred to a white, opaque 96-well plate. Into each well 25 µL of 1:10 ATP assay mix: ATP assay mix dilution buffer (Adenosine 5′-triphosphate (ATP) Bioluminescent Assay Kit, Sigma-Aldrich, Irvine, UK) was loaded. Luminescence was recorded following a 5s orbital mix using a FLOUstar OPTIMA (BMG Labtech, Ortenberg, Germany) luminometer. ATP concentration in each sample was calculated from a standard curve for all experiments (Faniku et al., 2018). Data is represented as the fold change in ATP concentration in the supernatant between control and treated cells.

2.7. ELISA

Culture supernatants were harvested following the treatments and assayed for IL-6 levels by ELISA assay (Quantikine® ELISA, RnDSystems, Abingdon, UK) according to the manufacturer's instructions. Absorbance was recorded at 450 nm and corrected to 570 nm using a FLOUstar OPTIMA plate reader (BMG Labtech, Ortenberg, Germany). The IL-6 concentration was calculated from a standard curve for all experiments. Data is represented as the fold change in IL-6 concentration in the supernatant between control and treated cells.

2.8. Statistical analysis

Experiments were performed in triplicate per setting and repeated on at least three separate occasions. All values indicate the mean ± SEM; the number of independent experiments is denoted by n. Data were compiled and analysed in GraphPad Prism 6 (GraphPad software, La

Jolla, San Diego, CA, USA). Statistical analysis was performed using Student's unpaired t-test or one-way ANOVA followed by Dunnett's as appropriate for data sets, detailed in figure legends. Statistical significance inferred at *P < 0.05; **P < 0.01; ***P < 0.001.

3. RESULTS

3.1. PGN from *S. aureus* induces changes in *IL6, IL8, CX26* and *TLR2* gene expression in HaCaT cells

To determine the impact of PGN isolated from *S. aureus* on gene expression profiles HaCaT cells were exposed to PGN for periods of 15 min to 24 h, followed by mRNA extraction and real time PCR analysis. IL-6 and IL-8 transcripts were examined as indicators of activation of pro-inflammatory signalling by PGN exposure. PGN treatment induced a potent up-regulation of both interleukin gene transcripts within 1-3 h of challenge (>50-fold increase, ****p<0.001*), which gradually reduced, with expression levels still >5-fold above basal levels at 24 h (Fig 1A, B). A transient increase in CX26 transcripts, peaking at 6 h, where expression was >10-fold above basal levels, and returning to basal levels after 24 h of exposure occurred (Fig 1C, ****p<0.001*). By contrast, CX43 transcripts were not induced (≤2-fold) above the threshold considered biologically significant (Dalman, 2012), during the 24 h PGN challenge (Fig 1D).

Inflammatory skin diseases are often characterised by hyperproliferation, for which Ki67 is a common cell proliferation marker (Li et al., 2015). The level of Ki67 gene expression was unchanged during 24 h PGN exposure, suggesting keratinocyte proliferation was not evoked by treatment with PGN (Fig 1E). TLR2 is a potential receptor that recognises PGN, triggering pro-inflammatory signalling events. TLR2 transcripts increased during 3 to 24 h of PGN challenge, peaking 6 h post exposure, confirming that TLR2 is part of the pro-inflammatory response enhanced by PGN in HaCaT cells (Fig 1F, **p<0.05*).

3.2. PGN from *S. aureus* differentially regulates CX43 and CX26 protein levels in keratinocytes

Immunostaining showed an increase in CX26 expression following 6-24 h exposure to PGN with increased protein distributed throughout the cytoplasm and at points of cell to cell contact on the plasma membrane (Fig 2 Ai-iii, supplementary Fig 1A, *p<0.05*). Immunostaining also confirmed the presence of CX43 at points of cell contact under normal conditions with a reduction of CX43 following 24 h PGN exposure evident (Fig 2Bi-iii).

An increase in CX26 protein expression following 3 h treatment with PGN was detected by western blot analysis (Fig 2C), consistent with gene transcript data (Fig 1C). Transfection of the cells with siRNA targeted to CX26 prevented the PGN induced CX26 expression (Fig 2C KD lanes). By contrast, western blot analysis further determined that CX43 protein levels were reduced ~50% following 24 h exposure to PGN, particularly levels of non-phosphorylated CX43 (P0) (Fig 2D, supplementary Fig 1 B, $p<0.005$).

3.3. *CX26* and *TLR2* siRNA knock-down and NF-kB blocking reduce PGN effects on *IL6* and *CX26* gene expression

To investigate the impact of *CX26, CX43* and *TLR2* on PGN induced responses these genes were knocked-down (KD) by delivery of siRNA targeted to *CX26, CX43* or *TLR2* respectively. The transfection efficiency of siRNA, determined by fluorescent microscopy analysis of the TYE 563^{TM} scrambled siRNA control was ~90% (data not shown). Twenty-four hours post transfection with each siRNA, mRNA was harvested and subject to RT-qPCR analysis to determine efficiency of gene knock-down under basal conditions. *CX26* expression was not reduced by siRNA-*CX26*, however this was predicted as under non-challenged conditions HaCaT cells express low levels of *CX26* (Supplementary Fig 2A). Expression of *CX43* was efficiently reduced following exposure to 5 nM siRNA targeted to CX43 (Supplementary Fig 2B). *TLR2* siRNA at 5 nM reduced *TLR2* mRNA levels around 50%, under these basal conditions (supplementary Figure 1C).

Subsequently, the cells were exposed to PGN for 3 h or 24 h prior to mRNA extraction and gene expression analysis. Following 3 h challenge with PGN *IL-6* expression was enhanced by ~30 fold over basal levels ($*p<0.05$), however KD of *CX26* or *TLR2* did not significantly influence this early event at the mRNA level (Fig 3A). By contrast, following 24 h exposure to PGN *CX26-KD* reduced the PGN-*IL-6* evoked response by ~50% ($^{+}p<0.05$) but *CX43* and *TLR2-KD* had no significant effect (Fig 3B).

Induction of *CX26* transcripts by PGN was significantly reduced by both *CX26*-KD and *TLR2*-KD following 3 h exposure to PGN (Fig 3C, $+p<0.05$), however this response was less at following 24 h exposure (Fig 3D).

TLR2 expression evoked by PGN was reduced by up to 80% following *TLR2*-KD and 3 h PGN exposure (Fig 3E, $^{+}p<0.05$). Following exposure to PGN for 24 h TLR2 remained at basal levels and it was not significantly affected by *TLR2*-KD (Fig 3F).

A key event in the TLR2 signalling pathway is the activation of NF-kB that acts as a transcription factor of the pro-inflammatory response. To determine the influence of NF-kB signalling on the PGN response HaCaT cells were pre-incubated with the NF-kB blocker BAY 11-7082 for 24 h followed by 3 h PGN exposure. This pre-treatment reduced the *IL-6* peak induced by PGN >50% and *CX26* peak >30% (Fig 4A and B, $+p<0.05$ and $++p<0.005$, respectively), but it did not change *CX43* gene expression levels (Fig 4C). These data confirm that the TLR2-NF-kB axis is one of the pathways which directly regulates *IL-6* and *CX26* gene expression.

3.4. PGN from *S. aureus* induces hemichannel activity and is regulated by CX26 and CX43

Hemichannel opening was assessed by measuring ATP release in the presence or absence of connexin channel blockers. As a positive control cells were deprived of calcium for 15 min which promoted hemichannel opening and ATP accumulation in the supernatant (>25-fold increase, $***p<0.001$). Pre-treatment with 50 μM CBX inhibited hemichannel opening induced by calcium deprivation, (Fig 5A, $^{++}p<0.005$). Acute exposure (15 min) of HaCaT cells to PGN also enhanced ATP release ($*p<0.01$), which was significantly reduced by co-incubation with 100 nM Gap26 (Fig 5B, $^{+}p<0.05$). ATP release induced by acute PGN exposure was also reduced by *CX26*- or *CX43*-KD ($^{+}p< 0.05$). *TLR2*-KD also showed a reduction in the PGN-induced ATP release, however this trend was not statistically significant to the PGN induced response (Fig 5C).

3.5. Release of IL-6 is reduced by CX channel blockers and TLR2-KD

The release of IL-6 from HaCaT cells following PGN challenge was determined by ELISA assays. HaCaT cells accumulated IL-6 in the supernatant during 24 h exposure to PGN (Fig 6A, $***p<0.001$). Exposure to the Cx channel blockers 50 μM CBX or 100 nM Gap27 alone did not influence basal IL-6 levels (Fig 6B and C). However, co-treatment with PGN and CBX or GAP27 significantly reduced the level of IL-6 release compared to PGN alone (Fig 6B and C, $^{+}p<0.05$ and $^{++}p<0.005$ respectively).

The IL-6 concentration in the supernatant was not affected by *CX26, CX43* or *TLR2* KD under non-challenged conditions (black columns), although *TLR2*-KD reduced the PGN evoked IL-6 response following 24 h (Fig 6D, $^{+}p<0.05$). CX26-KD inhibited the IL-6 response following

PGN challenge in multiple experiments (Fig 6D, *+p<0.05*). By contrast CX43-KD had no influence on the IL-6-PGN evoked response.

Finally, purinergic signalling blockers suramin (a general blocker) and A438079 (a P2X7R blocker) did not induce IL-6 accumulation in the supernatant in the absence of PGN. Pre-incubation with these blockers for 1 h followed by PGN exposure for 24 hours exhibited a trend towards inhibition of the IL-6 response induced by PGN (Fig 6E). The data further suggests that purinergic signalling contributes to maintaining IL-6 release under PGN challenge.

3.6. PANX1 does not play a role in the PGN induced pro-inflammatory response.

PANX1 is increasingly shown to be associated with purinergic signalling and pro-inflammatory mediated events (Crespo Yanguas et al., 2017). *PANX1* gene expression was not modified by PGN exposure throughout the 24 h challenge (Supplementary Fig 3A). Western blot and immunostaining analysis revealed no significant change in PANX1 protein expression during 24 h PGN treatment, and its distribution within the plasma membrane remained unaltered (Supplementary Fig 3 B-C).

Finally, to determine if PANX1 played a role in the PGN evoked response, ATP and IL-6 release were studied following reduction of *PANX1* expression by transfecting HaCaT cells with siRNA targeted to *PANX1*. This caused ~70% reduction in *PANX1* transcripts at 5 nM (Supplementary Fig 4A, ****p<0.001*). However, knock-down of PANX1 did not significantly change ATP release or IL-6 transcript levels (Supplementary Fig 4B and C).

4. Discussion

In the present work, we characterised connexin expression and activity during the pro-inflammatory response in keratinocytes. CX26 was acutely up-regulated following PGN challenge when it was used to simulate a pro-inflammatory environment. We determined for the first time in keratinocytes that this up-regulation is closely linked to the TLR2 signalling pathway by showing that TLR2 knockdown reduced CX26 PGN-induction and Cx hemichannel activity. Inhibition of connexin-hemichannel signalling or a reduction in *CX26* expression decreased the pro-inflammatory response in keratinocytes, as represented by the IL6 response to PGN. By contrast our studies determined that PANX1 does not play a significant role in the induction of this early innate immune response in keratinocytes and that prolonged exposure to PGN reduces CX43 protein expression. The data correlates with current

literature supporting the concept that enhanced CX26 expression and function is associated with a range of epidermal and epithelial pathologies (Chanson et al., 2018). We propose that the altered connexin balance elicited following PGN challenge evokes acute and long-term responses within the epidermis thereby influencing epidermal integrity. A summary of events is presented in Figure 7.

S. aureus is a Gram positive opportunistic pathogen of the skin and is associated with increased bacterial load in conditions such as psoriasis, atopic dermatitis, chronic non-healing wounds and KID syndrome (Sanford and Gallo, 2013). Upon infection with *S. aureus*, PGN within or released from the bacterial cell wall interacts with TLR2 receptors and triggers the innate immune response. This results in a signalling cascade that, through a first Ca^{2+} wave, ultimately activates NF-kB and its translocation to the nucleus where it acts as a transcription factor (Dunne and O'Neill, 2005). *CX26* mRNA expression was activated within one hour of exposure to PGN, in a similar timescale to *IL-6* and *IL-8*, suggesting similar regulation. Previous studies and promoter activity searches revealed that the *CX26* human promoter contains a potential binding site for NF-kB at -142bp relative to the translation start site (TSS) suggesting it is under a similar control mechanism to IL-6 and IL-8 (Dreos et al., 2017). Treatment of the cells with BAY11-7082, an inhibitor of NF-kB, reduced the PGN-evoked IL-6 and CX26 response but had no effect on CX43 expression. The increase in *CX26* gene expression was followed by an increase in CX26 protein expression, determined by western blot and immunofluorescence, within 3-6 h, with gene expression returning to basal levels by 24 h. It was noteworthy that neither *CX43* nor *PANX1* gene expression responded to PGN challenge at these timescales.

Up-regulation of CX26 is associated with several pathological skin conditions and is believed to be associated with elevated levels of inflammation. A recent psoriatic plaque transcriptome analysis identified *CX26* as one of the top 100 genes up-regulated (Li et al., 2014; Martin and van Steensel, 2015). The present data suggests that such up-regulation of CX26 expression throughout the epidermis may also result in enhanced hemichannel activity that might promote the defective differentiation of keratinocytes associated with psoriasis (Chanson et al., 2018). Observations in transgenic mice over-expressing CX26 in the suprabasal layer developed a hyperproliferative phenotype, similar to a number of epidermal human CX26 chanelopathies (Djalilian et al., 2006). An increase in CX26-hemichannel activity is related with inflammatory skin diseases as dominant mutations on the N-terminal tail or transmembrane-domain 2 evoke 'leaky' CX26-hemichannels, which is associated with the inflammatory condition KID syndrome (OMIM# 148210) (Donnelly et al., 2012; Garcia et al., 2015). Furthermore, in

chronic non-healing wound margins CX26 and Cx30 expression are up-regulated and are proposed to contribute to the inflammatory and proliferative status of the wound (Sutcliffe et al., 2015).

TLR2 is the prime receptor for PGN and is widely expressed in keratinocytes (Mempel et al., 2003). PGN interaction with TLR2 activates signalling cascades that induce expression of inflammatory cytokines and chemokines (Dunne and O'Neill, 2005; Ey et al., 2009). In HaCaT cells, *TLR2* gene expression was up-regulated by PGN exposure peaking after 6 h challenge. *IL-6* and *IL-8* were also acutely activated through the induction of the TLR2 signalling pathway. This was confirmed by siRNA inhibition of *TLR2* expression that reduced both *IL-6* gene expression and release following PGN exposure. *IL-6* gene expression and release after PGN challenge was also reduced by *CX26* KD, however CX43KD did not influence the PGN evoked response. The data suggest that CX26 may be an intermediate in PGN stimulation of *IL-6* expression, perhaps by communicating TLR2-Ca^{2+} fluxes which finally induce *IL-6* expression by NF-kB (Dunne and O'Neill, 2005; Ey et al., 2009). A similar mechanism of regulation between TLR2 and connexins was previously demonstrated in the airway epithelium where CX43-gap junctions were reported to be involved in the initial spread of TLR2-Ca^{2+} fluxes. The data from these studies strongly suggest that in the airway epithelium TLR2 stimulation induces acute changes in CX43 phosphorylation status and thereby gap junction activity (Ey et al., 2009; Martin and Prince, 2008).

There are a number of other examples reported in different tissues where TLR2 and connexin expression are linked. In endothelial cells the PGN-TLR2 axis regulated Cx43 expression and acutely evoked hemichannel activity (Robertson et al., 2010). TLR2 was also determined to modulate Cx43 synthesis and increase GJIC via CX43 during intestinal epithelial cell injury (Ey et al., 2009) and the PGN-TLR2 axis reduced *Cx43* and *Cx30* expression with an associated increase in *CX26* expression in astrocytes (Esen et al., 2007). In the present work the link between TLR2 and *CX26* in keratinocytes was confirmed by knocking-down *TLR2* expression which consequently prevented the induction of *CX26* gene expression following 3 h PGN challenge.

The PGN induced IL-6 response was not totally reduced following TLR2 knock-down, suggesting that other pathways are also involved. A role of extracellular ATP, connexin-hemichannels and purinergic receptors in inflammation and infectious disease has recently been recognized (Burnstock et al., 2012; Diezmos et al., 2016). ATP, a second messenger and

main purinergic messenger, is released into the extracellular space in apoptosis and inflammation by exocytosis, transporters and connexin-hemichannels (Eugenin, 2014). Previous studies in endothelial cells and HeLa cells expressing CX43 determined that PGN can acutely promote hemichannel opening (Robertson et al., 2010). In HaCaT cells transfected to express KID syndrome mutations PGN isolated from *S. aureus*, but not the skin commensal *S. epidermidis*, was also able to trigger hemichannel activity (Donnelly et al., 2012). Other bacterial cell wall components including lipopolysaccharide (LPS) from Gram negative bacterial cell walls, also augments astrocyte and microglial hemichannel opening and is reported to decrease gap junctional communication in liver and heart, (Eugenin, 2014; Lapato and Tiwari-Woodruff, 2018; Retamal et al., 2007a). The hemichannel opening triggered 15 min following exposure to PGN provides substantial evidence that connexin-hemichannel activity is involved in regulating the pro-inflammatory events evoked by PGN. In addition, ATP release was blocked by the general Cx-channel blocker CBX and connexin mimetic peptides Gap26 and Gap27. Connexin mimetic peptides (CMPs) are specific short sequences copied from connexin specific domains: Gap26 mimics the sequence of the extracellular loop 1 and Gap27 the extracellular loop 2 of CX43. Both have been widely used to inhibit Cx mediated signalling events in diverse tissue networks (Willebrords et al., 2017). We have recently reported that Gap27 is effective in inhibiting ATP release from keratinocytes at concentrations of 100 nM, where it promotes keratinocyte migration with limited effect on proliferation (Faniku et al., 2018). Gap27 is reported to be specific for CX43 and Cx37 by several groups (Martin et al., 2005). This suggests that CX43 signalling plays a role in the acute term response elicited in keratinocytes following PGN challenge. Gap26 has a broader connexin specificity, and is also reported to be a more effective hemichannel inhibitor that Gap27, which may explain the slightly greater reduction in ATP release observed following PGN challenge (Desplantez et al., 2012; Wright et al., 2009). In cell migration studies previously performed in keratinocytes and fibroblasts, Gap26 was also slightly more efficient than Gap27 in keratinocytes which was attributed to the broader inhibitory capacity of this peptide (Wright et al., 2009). Whether the acute ATP release triggered within 15 min exposure to PGN is due to CX43 or CX26-hemichannels in keratinocytes is difficult to determine without highly selective CX26-hemichannel blockers; nevertheless, *CX26* and *CX43* knock-down reduced the ATP-peak induced by PGN, which confirms that both connexins are involved in this response.

Keratinocytes are reported to release ATP in a critical gradient dependent manner reflecting the differentiation status of the cells, with connexin signaling reported to play a role in the upper stratified layers, where CX26 tends to be spatially expressed (Tsutsumi et al., 2009). Most Cx-hemichannels are closed under 'standard' conditions, however CX26-hemichannels are an exception and human and sheep CX26 hemichannels are reported to form open voltage-gated hemichannels under resting conditions (Gonzalez et al., 2006). The fact that following pro-inflammatory challenge CX26 expression is so dramatically upregulated suggests that the CX26 hemichannels produce an excessive release of ATP, which activates excitatory purinergic receptors of neighbouring cells. Thus overexpression of CX26 will alter basal ATP release levels and impact on pro-inflammatory events and differentiation programmes. Indeed, the present data further determined that the enhanced levels of CX26 and hemichannel activity within keratinocytes are linked with the trigger of inflammation because reduction of CX26 expression and inhibition of hemichannel activity by using connexin-channel blockers dramatically decreased PGN-induced *IL-6* expression. By contrast siRNA targeted to CX43 had limited effect.

Although an increase in CX43 expression was reported in endothelial cells following PGN challenge no changes in *CX43* gene expression in keratinocytes was observed during PGN exposure. In endothelial cells *Cx43* gene expression was increased 6 h following PGN challenge, but no overall decrease in Cx43 was observed following 24 h exposure (Robertson et al., 2010). By contrast in the present study in keratinocytes a small increase in *CX43* gene expression was observed 15 min following PGN exposure but this was not above the two-fold increase and therefore not significant. Instead, immunofluorescence and western blot analysis determined an overall decrease in CX43 protein expression during the 24 h PGN exposure suggesting targeted degradation of the protein and this warrants further investigation.

The mimetic peptide Gap27 targeting CX43 reduced IL-6 release in HaCaT cells, although not to the same extent as the generic channel blocker CBX, suggesting that other channels are involved in regulating these signalling pathways. Given the identification of a significant role for CX26 in the pro-inflammatory events we propose that initial localized events, triggered by PGN/TLR2 interactions contribute to the 'acute' innate immune trigger. As this trigger also results in enhancing CX26 levels we propose that the longer term responses are attributed to CX26 channel activity, particularly in chronically inflamed epidermal tissue where the expression of CX26 is exacerbated. A role for connexin signaling in chronic inflammation is receiving increased attention in diverse tissue networks (Kim et al., 2016; Willebrords et al.,

2016). A range of peptides targeting CX43 clearly reduce inflammation and scarring in various systems including the skin and the cornea (Willebrords et al., 2017). The success of such peptides in translational research is highlighted by the Phase 3 clinical trial status for chronic non-healing wounds of ACT-1 (https://firststringresearch.com/) and on-going clinical reports by Ocunexus (https://ocunexus.com/).

Pannexins, sister proteins to the connexins, sharing common topological membrane organization and channel formation with connexins are also increasingly associated with inflammatory mediated events and recruitment of the inflammasome. PANX1 has been shown to be involved in ATP release driving inflammation by assisting in the activation of inflammasomes, the release of pro-inflammatory cytokines and the activation and migration of leukocytes (Crespo Yanguas et al., 2017). PANX1 and Panx3 are expressed in keratinocytes and are proposed to have a complementary role to the connexins (Celetti et al., 2010). In the present work PANX1 was clearly expressed at the plasma membrane in HaCaT cell. ATP release via PANX1, is known to act as a paracrine transmitter and activates P2 receptors, such as P2X7R, this is followed by activation of an inflammatory response in immune cells with subsequent release of cytokines. However, the present data suggests that in keratinocytes PANX1 does not participate in the acute PGN/TLR2 pro-inflammatory response, as PANX1 gene and protein expression levels were not modified following PGN exposure and siRNA targeted to PANX1 did not influence PGN evoked ATP or IL-6 release. By contrast inhibition of purinergic receptor signalling reduced the PGN-IL-6 evoked response, confirming an important role for purinergic signalling in the process.

In conclusion, HaCaT cells provide a valuable model for investigating the role of connexins in the epidermal innate immune response. The time courses of mRNA induction of IL-6, TLR2 and CX26 following PGN challenge and the effects of knocking down TLR2 and CX26 indicate both IL6 and CX26 are targets of TLR2 activation in HaCaT cells. At the protein level, our data points towards a significant role for connexin channel function influencing IL6 release. However, the acute nature of this response suggests that it does not involve CX26 alone, but that another connexin, probably CX43 is involved. As CX43 is decreased at later timepoints we propose that the overexpression of CX26 in chronically inflamed keratinocytes may contribute to the exacerbated release of ATP that consequently further stimulates purinergic signalling and sustained inflammation. The acute response, may also trigger CX43 hemichannel activity, but unlike other tissues, in keratinocytes this evokes the internalization of CX43 into the cytoplasm and ultimately reduces CX43 protein expression. As CX26 does

not interact with the cytoskeleton allowing cell plasticity, we propose the exacerbated hemichannel activity will also remodel critical ATP-Ca^{2+} gradients within the epidermis and trigger altered proliferation and differentiation of keratinocytes. Thus a chronically inflamed epidermis has an altered connexin balance that influences epidermal integrity and highlights that both CX26 and CX43 are prime therapeutic targets for inflammatory skin disease. By contrast our data suggest that PANX1 does not participate in the pro-inflammatory response induced by *S. aureus* in keratinocytes. Future work is required to dissect these events further.

ACKNOWLEDGMENTS

We thank Zealand Pharma for the supply of Gap27 used in this study. We are indebted to Professor Malcolm Hodgins for continued support and comment and to Edward Leithe, Oslo University Hospital, Norway, for the supply of the Connexin43 antibody.

FUNDING STATEMENT

LGV was supported by a GCU PhD studentship, EO by a PhD studentship from the Psoriasis Association (ST3 15) and AJ by a scholarship from the Saudi Government.

CONFLICT OF INTEREST

The authours declare that there is no conflict of interest

AUTHORS' CONTRIBUTIONS

LGV wrote the manuscript, planned and carried out the majority of the experiments with inputs from EO and AJ. PEM directed the research and collated the final version of the manuscript and CB contributed to data analysis and final proof reading**.**

REFERENCES

Baroni A, Buommino E, De Gregorio V, Ruocco E, Ruocco V, Wolf R. 2012. Structure and function of the epidermis related to barrier properties. Clin Dermatol 30(3):257-262.

Boukamp P, Petrussevska RT, Breitkreutz D, Hornung J, Markham A, Fusenig NE. 1988. Normal keratinization in a spontaneously immortalized aneuploid human keratinocyte cell line. J Cell Biol 106(3):761-771.

Brandner JM, Houdek P, Husing B, Kaiser C, Moll I. 2004. Connexins 26, 30, and 43: differences among spontaneous, chronic, and accelerated human wound healing. J Invest Dermatol 122(5):1310-1320.

Burnstock G, Knight GE, Greig AV. 2012. Purinergic signaling in healthy and diseased skin. J Invest Dermatol 132(3):526-546.

Ceelen L, Haesebrouck F, Vanhaecke T, Rogiers V, Vinken M. 2011. Modulation of connexin signaling by bacterial pathogens and their toxins. Cell Mol Life Sci 68(18):3047-3064.

Celetti SJ, Cowan KN, Penuela S, Shao Q, Churko J, Laird DW. 2010. Implications of pannexin 1 and pannexin 3 for keratinocyte differentiation. J Cell Sci 123(Pt 8):1363-1372.

Chanson M, Watanabe M, O'Shaughnessy EM, Zoso A, Martin PE. 2018. Connexin Communication Compartments and Wound Repair in Epithelial Tissue. Int J Mol Sci 19(5).

Crespo Yanguas S, Willebrords J, Johnstone SR, Maes M, Decrock E, De Bock M, Leybaert L, Cogliati B, Vinken M. 2017. Pannexin1 as mediator of inflammation and cell death. Biochim Biophys Acta 1864(1):51-61.

Dalman M. 2012. Fold change and p-value cutoffs significantly alter microarray interpretations. BMC bioinformatics, 13 (Suppl 2):S11.

Desplantez T, Verma V, Leybaert L, Evans WH, Weingart R. 2012. Gap26, a connexin mimetic peptide, inhibits currents carried by connexin43 hemichannels and gap junction channels. Pharmacol Res 65(5):546-552.

Di WL, Rugg EL, Leigh IM, Kelsell DP. 2001. Multiple epidermal connexins are expressed in different keratinocyte subpopulations including connexin 31. J Invest Dermatol 117(4):958-964.

Diezmos EF, Bertrand PP, Liu L. 2016. Purinergic Signaling in Gut Inflammation: The Role of Connexins and Pannexins. Front Neurosci 10:311.

Djalilian AR, McGaughey D, Patel S, Seo EY, Yang C, Cheng J, Tomic M, Sinha S, Ishida-Yamamoto A, Segre JA. 2006. Connexin 26 regulates epidermal barrier and wound remodeling and promotes psoriasiform response. J Clin Invest 116(5):1243-1253.

Donnelly S, English G, de Zwart-Storm EA, Lang S, van Steensel MA, Martin PE. 2012. Differential susceptibility of CX26 mutations associated with epidermal dysplasias to peptidoglycan derived from Staphylococcus aureus and Staphylococcus epidermidis. Exp Dermatol 21(8):592-598.

Dreos R, Ambrosini G, Groux R, Cavin Perier R, Bucher P. 2017. The eukaryotic promoter database in its 30th year: focus on non-vertebrate organisms. Nucleic Acids Res 45(D1):D51-D55.

552 Dunne A, O'Neill LA. 2005. Adaptor usage and Toll-like receptor signaling specificity. FEBS
553 letters 579(15):3330-3335.
554 Esen N, Shuffield D, Syed MM, Kielian T. 2007. Modulation of connexin expression and gap
555 junction communication in astrocytes by the gram-positive bacterium S. aureus. Glia
556 55(1):104-117.
557 Eugenin EA. 2014. Role of connexin/pannexin containing channels in infectious diseases.
558 FEBS letters 588(8):1389-1395.
559 Ey B, Eyking A, Gerken G, Podolsky DK, Cario E. 2009. TLR2 mediates gap junctional
560 intercellular communication through connexin-43 in intestinal epithelial barrier injury.
561 J Biol Chem 284(33):22332-22343.
562 Faniku C, O'Shaughnessy E, Lorraine C, Johnstone SR, Graham A, Greenhough S, Martin
563 PEM. 2018. The Connexin Mimetic Peptide Gap27 and CX43-Knockdown Reveal
564 Differential Roles for Connexin43 in Wound Closure Events in Skin Model Systems.
565 Int J Mol Sci 19(2).
566 Garcia IE, Bosen F, Mujica P, Pupo A, Flores-Munoz C, Jara O, Gonzalez C, Willecke K,
567 Martinez AD. 2016. From Hyperactive Connexin26 Hemichannels to Impairments in
568 Epidermal Calcium Gradient and Permeability Barrier in the Keratitis-Ichthyosis-
569 Deafness Syndrome. J Invest Dermatol 136(3):574-583.
570 Garcia IE, Maripillan J, Jara O, Ceriani R, Palacios-Munoz A, Ramachandran J, Olivero P,
571 Perez-Acle T, Gonzalez C, Saez JC, Contreras JE, Martinez AD. 2015. Keratitis-
572 ichthyosis-deafness syndrome-associated CX26 mutants produce nonfunctional gap
573 junctions but hyperactive hemichannels when co-expressed with wild type CX43. J
574 Invest Dermatol 135(5):1338-1347.
575 Gonzalez D, Gomez-Hernandez JM, Barrio LC. 2006. Species specificity of mammalian
576 connexin-26 to form open voltage-gated hemichannels. FASEB J 20(13):2329-2338.
577 Holland DB, Bojar RA, Farrar MD, Holland KT. 2009. Differential innate immune responses
578 of a living skin equivalent model colonized by Staphylococcus epidermidis or
579 Staphylococcus aureus. FEMS Microbiol Lett 290(2):149-155.
580 Jiang C, Xu M, Kuang X, Xiao J, Tan M, Xie Y, Xiao Y, Zhao F, Wu Y. 2017. Treponema
581 pallidum flagellins stimulate MMP-9 and MMP-13 expression via TLR5 and
582 MAPK/NF-kappaB signaling pathways in human epidermal keratinocytes. Exp Cell
583 Res 361(1):46-55.
584 Kam E, Melville L, Pitts JD. 1986. Patterns of junctional communication in skin. J Invest
585 Dermatol 87(6):748-753.
586 Kim Y, Davidson JO, Gunn KC, Phillips AR, Green CR, Gunn AJ. 2016. Role of
587 Hemichannels in CNS Inflammation and the Inflammasome Pathway. Advances in
588 protein chemistry and structural biology 104:1-37.
589 Labarthe MP, Bosco D, Saurat JH, Meda P, Salomon D. 1998. Upregulation of connexin 26
590 between keratinocytes of psoriatic lesions. J Invest Dermatol 111(1):72-76.
591 Laird DW. 2006. Life cycle of connexins in health and disease. Biochem J 394(Pt 3):527-543.
592 Lapato AS, Tiwari-Woodruff SK. 2018. Connexins and pannexins: At the junction of neuro-
593 glial homeostasis & disease. J Neurosci Res 96(1):31-44.
594 Lee WK, Choi SW, Lee HR, Lee EJ, Lee KH, Kim HO. (2001). Purinoceptor-mediated calcium
595 mobilization and proliferation in HaCaT keratinocytes. J Dermatol Sci 25(2):97-105

596 Leithe E, Rivedal E. 2004. Ubiquitination and down-regulation of gap junction protein
597 connexin-43 in response to 12-O-tetradecanoylphorbol 13-acetate treatment. J Biol
598 Chem 279(48):50089-50096.
599 Li B, Tsoi LC, Swindell WR, Gudjonsson JE, Tejasvi T, Johnston A, Ding J, Stuart PE, Xing
600 X, Kochkodan JJ, Voorhees JJ, Kang HM, Nair RP, Abecasis GR, Elder JT. 2014.
601 Transcriptome analysis of psoriasis in a large case-control sample: RNA-seq provides
602 insights into disease mechanisms. J Invest Dermatol 134(7):1828-1838.
603 Li LT, Jiang G, Chen Q, Zheng JN. 2015. Ki67 is a promising molecular target in the diagnosis
604 of cancer (review). Mol Med Rep 11(3):1566-1572.
605 Livak KJaS, T.D., . 2001. Analysis of Relative Gene Expression Data Using Real- Time
606 Quantitative PCR and the 2 ⁻ □□ C T Method. Methods 25:.402–408.
607 Lucke T, Choudhry R, Thom R, Selmer IS, Burden AD, Hodgins MB. 1999. Upregulation of
608 connexin 26 is a feature of keratinocyte differentiation in hyperproliferative epidermis,
609 vaginal epithelium, and buccal epithelium. J Invest Dermatol 112(3):354-361.
610 Mankus C, Rich C, Minns M, Trinkaus-Randall V. (2011). Corneal epithelium expresses a
611 variant of P2X(7) receptor in health and disease. PLoS One 6(12):e28541.
612 Martin FJ, Prince AS. 2008. TLR2 regulates gap junction intercellular communication in
613 airway cells. J Immunol 180(7):4986-4993.
614 Martin PE, Easton JA, Hodgins MB, Wright CS. 2014. Connexins: sensors of epidermal
615 integrity that are therapeutic targets. FEBS letters 588(8):1304-1314.
616 Martin PE, van Steensel M. 2015. Connexins and skin disease: insights into the role of beta
617 connexins in skin homeostasis. Cell Tissue Res 360(3):645-658.
618 Martin PE, Wall C, Griffith TM. 2005. Effects of connexin-mimetic peptides on gap junction
619 functionality and connexin expression in cultured vascular cells. Br J Pharmacol
620 144(5):617-627.
621 Mempel M, Voelcker V, Kollisch G, Plank C, Rad R, Gerhard M, Schnopp C, Fraunberger P,
622 Walli AK, Ring J, Abeck D, Ollert M. 2003. Toll-like receptor expression in human
623 keratinocytes: nuclear factor kappaB controlled gene activation by Staphylococcus
624 aureus is toll-like receptor 2 but not toll-like receptor 4 or platelet activating factor
625 receptor dependent. J Invest Dermatol 121(6):1389-1396.
626 Retamal MA, Froger N, Palacios-Prado N, Ezan P, Saez PJ, Saez JC, Giaume C. 2007a. CX43
627 hemichannels and gap junction channels in astrocytes are regulated oppositely by
628 proinflammatory cytokines released from activated microglia. J Neurosci
629 27(50):13781-13792.
630 Retamal MA, Schalper KA, Shoji KF, Bennett MV, Saez JC. 2007b. Opening of connexin 43
631 hemichannels is increased by lowering intracellular redox potential. Proc Natl Acad Sci
632 USA 104(20):8322-8327.
633 Robertson J, Lang S, Lambert PA, Martin PE. 2010. Peptidoglycan derived from
634 Staphylococcus epidermidis induces Connexin43 hemichannel activity with
635 consequences on the innate immune response in endothelial cells. Biochem J
636 432(1):133-143.
637 Sanford JA, Gallo RL. 2013. Functions of the skin microbiota in health and disease. Semin
638 Immunol 25(5):370-377.

Shuja Z, Li L, Gupta S, Mese G, White TW. 2016. Connexin26 Mutations Causing Palmoplantar Keratoderma and Deafness Interact with Connexin43, Modifying Gap Junction and Hemichannel Properties. J Invest Dermatol 136(1):225-235.

Sutcliffe JE, Chin KY, Thrasivoulou C, Serena TE, O'Neil S, Hu R, White AM, Madden L, Richards T, Phillips AR, Becker DL. 2015. Abnormal connexin expression in human chronic wounds. Br J Dermatol 173(5):1205-1215.

Taylor SC, Berkelman T, Yadav G, Hammond M. 2013. A defined methodology for reliable quantification of Western blot data. Mol Biotechnol 55(3):217-226.

Tsutsumi M, Denda S, Inoue K, Ikeyama K, Denda M. 2009. Calcium ion gradients and dynamics in cultured skin slices of rat hindpaw in response to stimulation with ATP. J Invest Dermatol 129(3):584-589.

Willebrords J, Crespo Yanguas S, Maes M, Decrock E, Wang N, Leybaert L, Kwak BR, Green CR, Cogliati B, Vinken M. 2016. Connexins and their channels in inflammation. Crit Rev Biochem Mol Biol 51(6):413-439.

Willebrords J, Maes M, Crespo Yanguas S, Vinken M. 2017. Inhibitors of connexin and pannexin channels as potential therapeutics. Pharmacol Ther.

Wright CS, van Steensel MA, Hodgins MB, Martin PE. 2009. Connexin mimetic peptides improve cell migration rates of human epidermal keratinocytes and dermal fibroblasts in vitro. Wound Repair Regen 17(2):240-249.

Figure Legends

Figure 1: Changes in gene expression following PGN challenge.
HaCaT cells were challenged with 10 µg/mL PGN for 15 min, 1, 3, 6 and 24 h prior to mRNA extraction and RT-PCR analysis to determine A) *IL-6*, B) *IL-8*, C) *CX26*, D) *CX43*, E) *Ki67* and F) *TLR2* gene expression profiles. Results are expressed as the fold increase in target gene expression over the housekeeping gene GAPDH compared to non-challenged cells (n=4). Statistical analysis performed using one-way ANOVA and Dunnet's multiple comparison test compared to control, $*p<0.05$, $**p<0.005$, $***p<0.001$. Red dotted line indicates +2-fold increase threshold and blue dotted line indicates -2-fold reduction threshold.

Figure 2: Cx26 and Cx43 protein expression following 3-24 h PGN exposure.
Ai-iii) Cx26 representative immunostaining under control conditions and following 6-24 h PGN challenge. Bi-iii) Cx43 representative immunostaining under control conditions and following 6-24 h PGN challenge. Arrows indicate punctate connexin staining at the cell membrane. Bar = 10µm. C) Representative Cx26 western blot under control conditions and following 3 h PGN challenge. Note the absence of Cx26 in samples exposed to siRNA targeted to Cx26 (KD). D) CX43 representative blot under control conditions and following 6 and 24 h PGN exposure. Note the reduction in Cx43 at 24 h. GAPDH loading control. Representative blots of n=5.

Figure 3: Gene expression following siRNA knock-down and 3-24 h PGN.
HaCaT cells were transfected with siRNA targeted to *Cx26, Cx43* and *TLR2* 24 h prior to challenge with PGN for 3 or 24 h in order to determine A, B) *IL-6;* C, D) *Cx26*; E, F) *TLR2* gene expression levels. Results are expressed as the fold change in target gene expression over the housekeeping gene GAPDH compared to cells transfected with scrambled siRNA control. N=3, statistical analysis performed using t-test compared to control, $*p<0.05$ and $***p<0.001$ and t-test compared to PGN treated $+p<0.05$. Red dotted line indicates +2-fold increase threshold and blue dotted line indicates -2-fold reduction threshold.

Figure 4: Changes in gene expression following NF-kβ blocking and PGN challenge.
HaCaT cells were pre-blocked with BAY 11-7082 for 24 h and challenged with PGN 3 h prior to mRNA extraction and RT-qPCR analysis to determine A) *IL-6*; B) *CX26* and C) *CX43* gene expression profiles. Results are expressed as the fold increase in target gene expression over the housekeeping gene GAPDH compared to non-challenged cells (n=3). Statistical analysis was performed using one-way ANOVA and Dunnet's multiple comparison test to compare PGN treated to control, $*p<0.05$, $***p<0.001$ and t-test to compare PGN challenged and BAY 11-7082+PGN treated cells respectively, $+p<0.05$, $++P<0.005$. Red dotted line indicates +2-fold increase threshold and blue dotted line indicates -2-fold reduction threshold.

Figure 5: ATP release following challenge of HaCaT cells with zero Calcium or PGN.
HaCaT cells were subject to: A)15 min exposure to Ca^{2+} free conditions in the presence or absence of 50 µM CBX; B) PGN for 15 min in the presence or absence of 100nM Gap26 or Gap27; C) siRNA-KD of Cx26, Cx43 and TLR2 24 h prior to challenge with 15 min PGN; prior to harvesting media and ATP analysis. Results are expressed as the fold increase in ATP concentration in the media compared to control cells (n=6). Significant differences determined

using one-way ANOVA followed by Dunnet's multiple comparison analysis. **p<0.05; ***p<0.001* compared to non-challenged control and t-test *+p<0.05; ++p<0.005* compared to challenged cells to pre-blocked or KD samples.

Figure 6: IL-6 release in the presence or absence of PGN, Cx blockers and/or purinergic blockers.
The media from HaCaT cells was harvested and IL-6 levels determined by ELISA. A) HaCaT cells were exposed to 15min-24h PGN challenge. B) They were pre-treated with CBX for 1h and/or challenged with PGN for 6h. C) They were pre-treated with Gap27 for 1h and/or challenged with PGN for 6h. D) HaCaT cells were transfected with siRNA targeted *Cx26, Cx43* and *TLR2* 24h prior to challenge with PGN for 24 h. E) HaCaT cells were pre-treated with Suramin or A438079 1 h and PGN for 24 h (n=3). Data is presented as fold change of IL-6 concentration in the supernatant in treated cells over control. Significant differences determined using one-way ANOVA followed by Dunnet's multiple comparison analysis **p<0.05, **p<0.005 and ***p<0.001* compared to non-challenged control and t-test *+p<0.05* and *++p<0.005* compared treated with blocker-PGN or KD-PGN to treated cells with PGN only.

Figure 7: Schematic representation of the proposed pathway linking Cx channel function and innate immunity in keratinocytes.
(1) PGN from *S. aureus* interacts with TLR2 and produces an acute pro-inflammatory response and triggers hemichannel activity, releasing ATP from the cell within 15 min of challenge. (2) It also triggers intracellular signalling pathways that induce expression of Cx26 and IL-6. (4). (5) Overexpression of Cx26 increases ATP release, which activates purinergic signalling. (6) Purinergic signalling triggers subsequent signalling cascades maintaining a longer pro-inflammatory response. (7) The longer-term interaction between PGN and TLR2 also induces the relocation and potential degradation of Cx43.

Supplementary Figures

Supplementary Figure 1: Exposure to PGN has differential effects on Cx26 and Cx43 protein expression and spatial localisation. A: HaCaT cells were exposed to PGN for 6 or 24 h followed by fixation and immunocytochemical analysis using an antibody targeting Cx26 (green). Histogram A represents semi-quantitative pixel intensity levels of Cx26 staining compared to non-challenged control (n=5). B: HaCaT cells were exposed to PGN for 6 and 24 h prior to harvesting protein and subject to SDS PAGE and Western blot analysis using an antibody targeted to Cx43. Histogram B represents Cx43 expression extracted from image density analysis (n=5). Significant differences determined using ANOVA and Dunnet's multiple comparison compared with the control **p<0.05; **p <0.01.*

Supplementary Figure 2: siRNA dose response.
HaCaT cell were transfected with siRNA at different concentrations 24 h prior to mRNA extraction and RT-qPCR analysis to determine A) Cx26, B) Cx43 and C) TLR2 gene expression profiles. Results are expressed as fold change in target gene expression over the housekeeping gene GAPDH compared to cells transfected with scrambled siRNA control. N=3, statistical analysis performed using one-way ANOVA and Dunnet's multiple comparison

test compared to control, **p<0.005 and ***p<0.001. Blue dotted line indicates -2-fold reduction threshold.

Supplementary Figure 3: Panx1 gene and protein expression under PGN challenge.
HaCaT cells were treated with PGN for 15 min to 24 h. A) Panx1 mRNA levels. Results are expressed as the fold increase in target gene expression over the housekeeping gene GAPDH compared to non-challenged cells (n=3). Statistical analysis performed using one-way ANOVA and Dunnet's multiple comparison compared treated to control, *$p<0.005$, ***$p<0.001$. B) Panx1 protein expression analysed by western blot and representative blot. Results are expressed as the fold increase in treated over to non-challenged cells. n=5, statistical analysis performed using one-way ANOVA and Dunnet's multiple comparison test compared to control. C) Panx1 representative immunostaining. Bar= 10μm

Supplementary Figure 4: Effects of Panx1 on the PGN response.
A) *Panx1* mRNA levels following siRNA against *Panx1* transfection. Results are expressed as the fold increase in target gene expression over the housekeeping gene GAPDH compared to non-challenged cells (n=3). Statistical analysis performed using one-way ANOVA and Dunnet's multiple comparison compared treated to control, **$p<0.005$, ***$p<0.001$. Blue dotted line indicates -2-fold reduction threshold. B) Fold change in ATP concentration in the supernatant following 24 h *Panx1*-KD and/or 15 min PGN (n=9). C) Fold change in IL-6 concentration in the supernatant following 24 h Panx1-KD and/or 24h PGN (n=3). Data represented as fold change of the concentration of ATP or IL-6 in the supernatant in treated cells compared to untreated cells. Statistical analysis was also performed using t-test to compare treated to control cells.

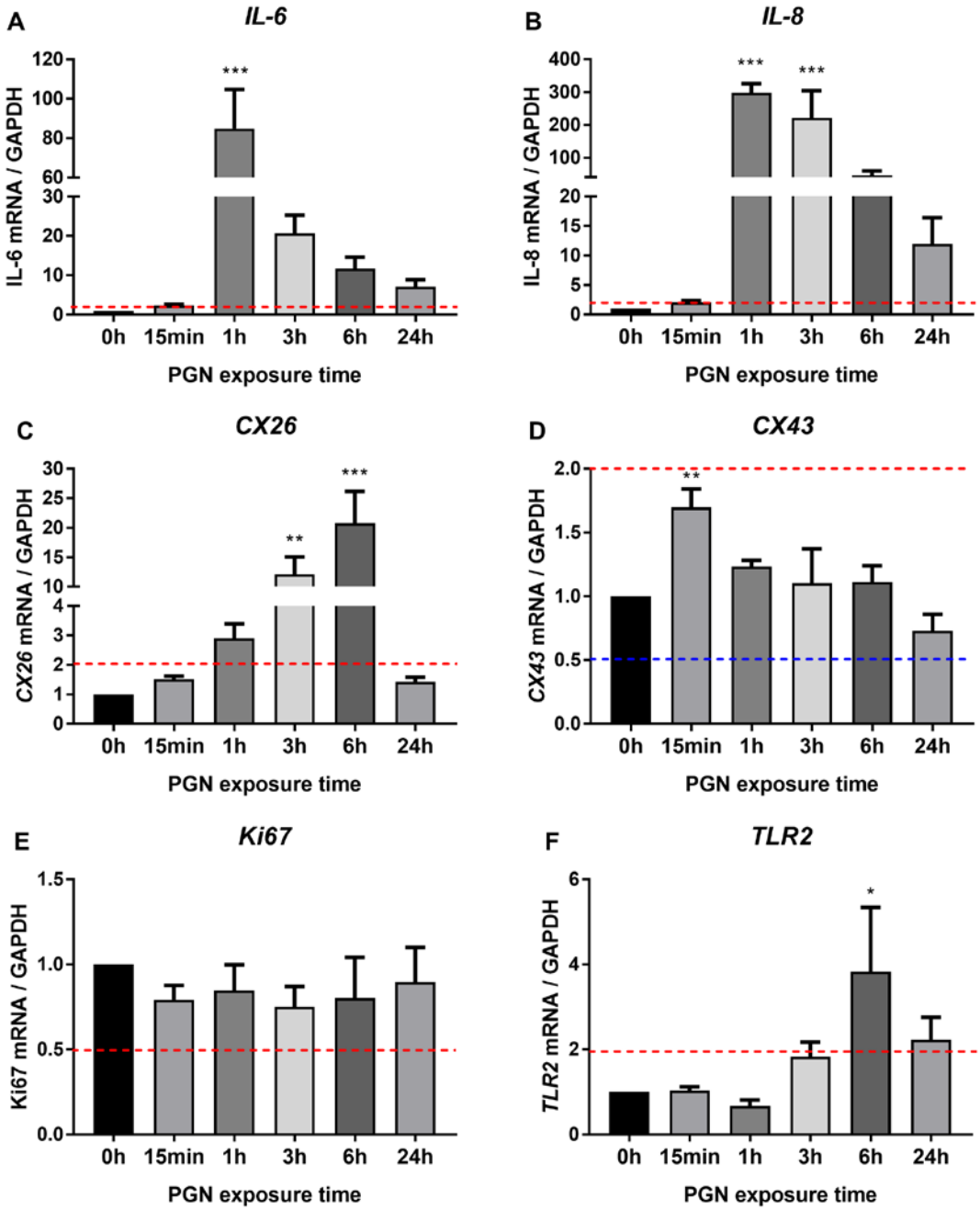

773

774 Figure 1

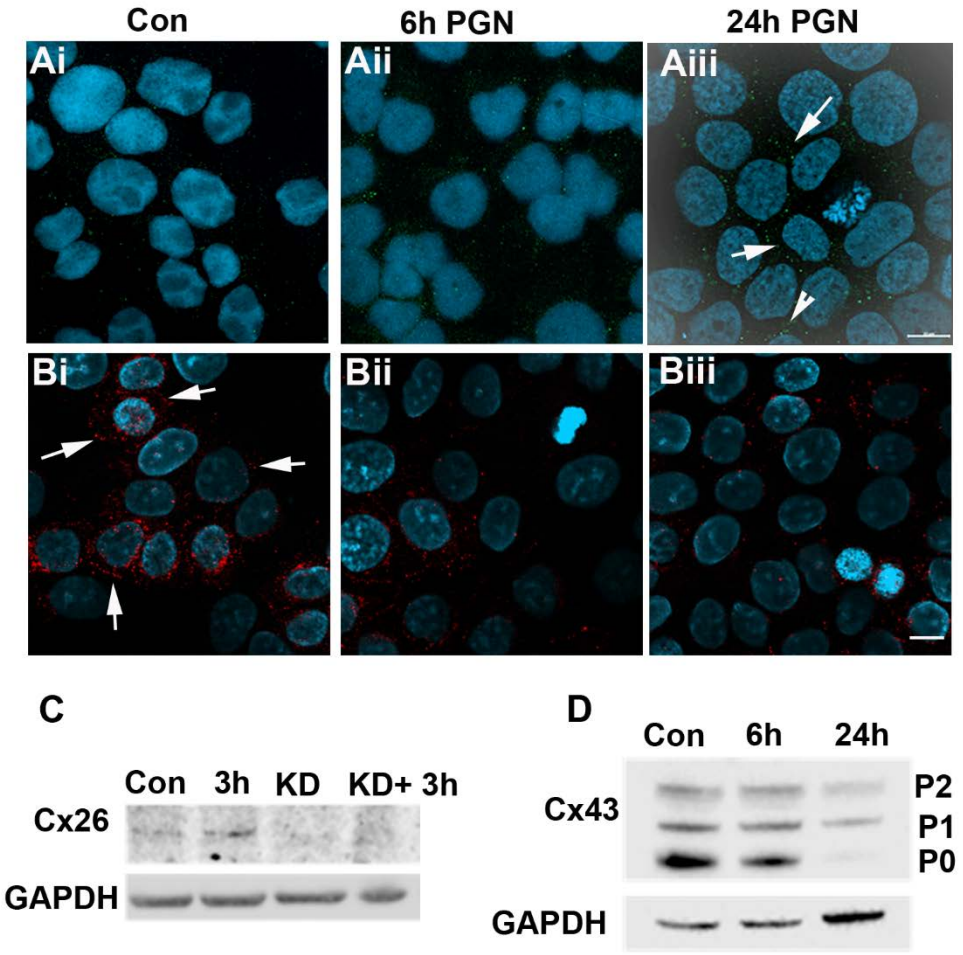

775

776 Figure 2

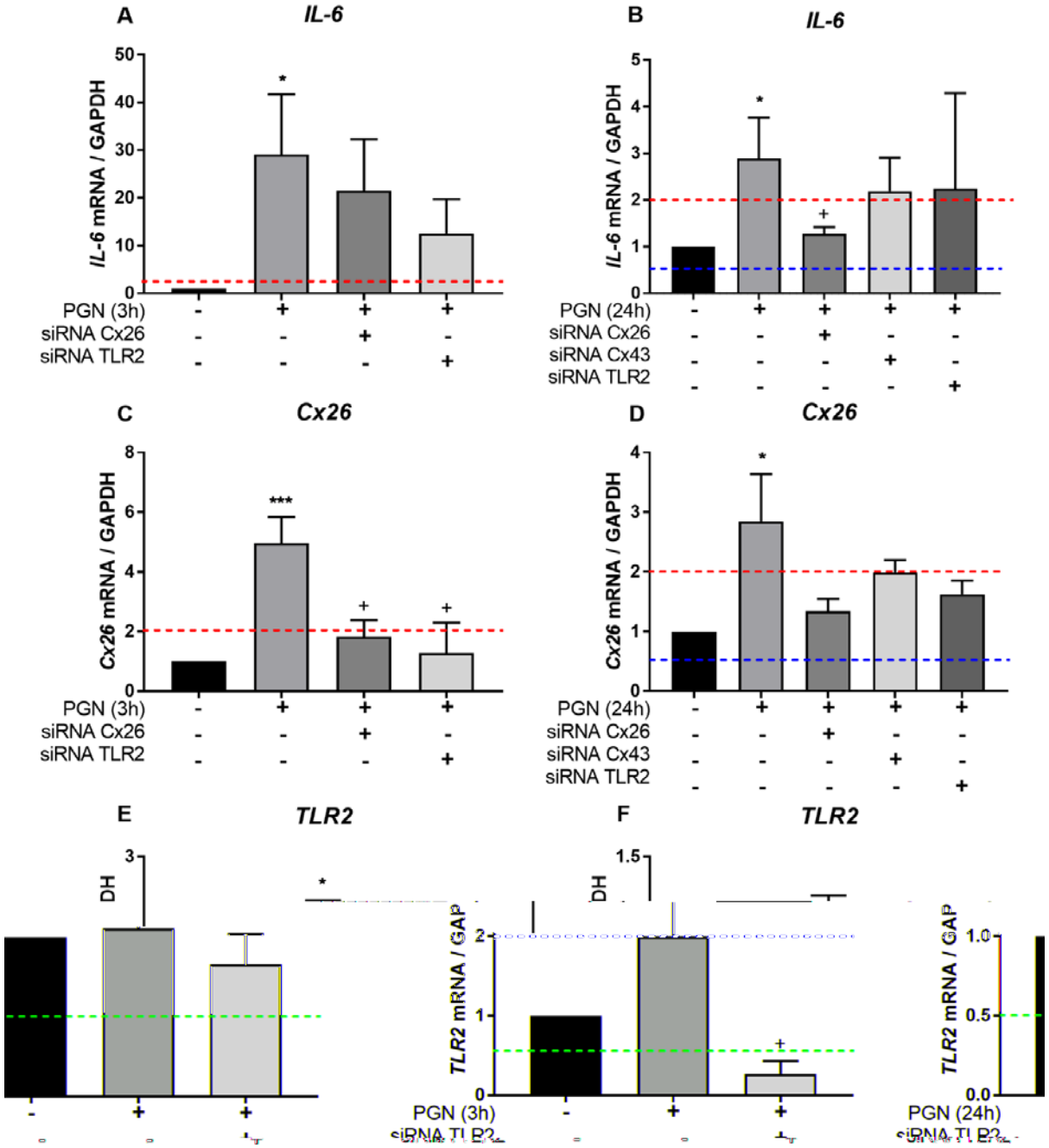

777

778 Figure 3

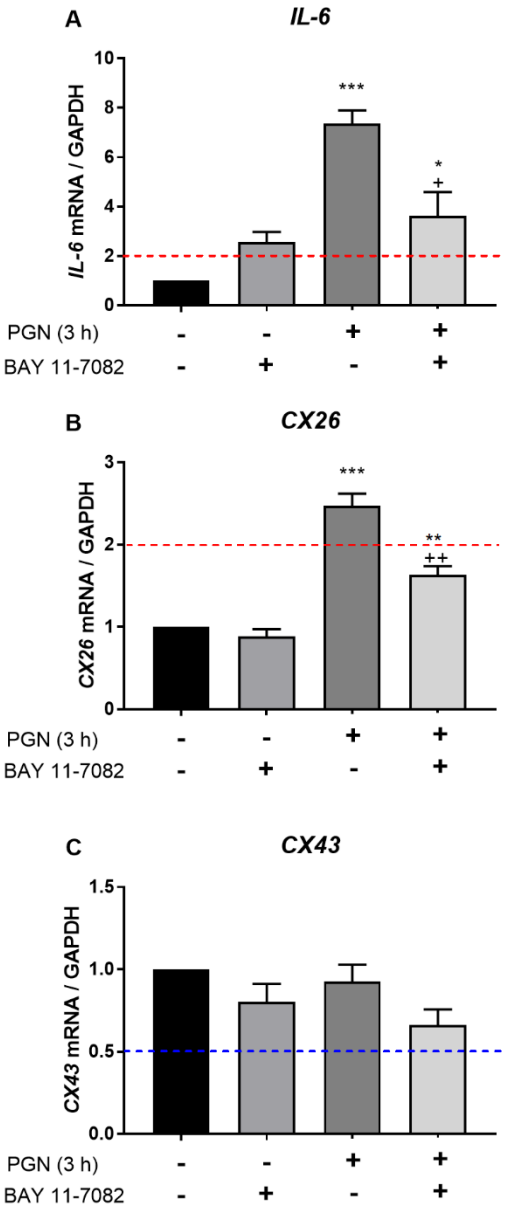

779

780 Figure 4

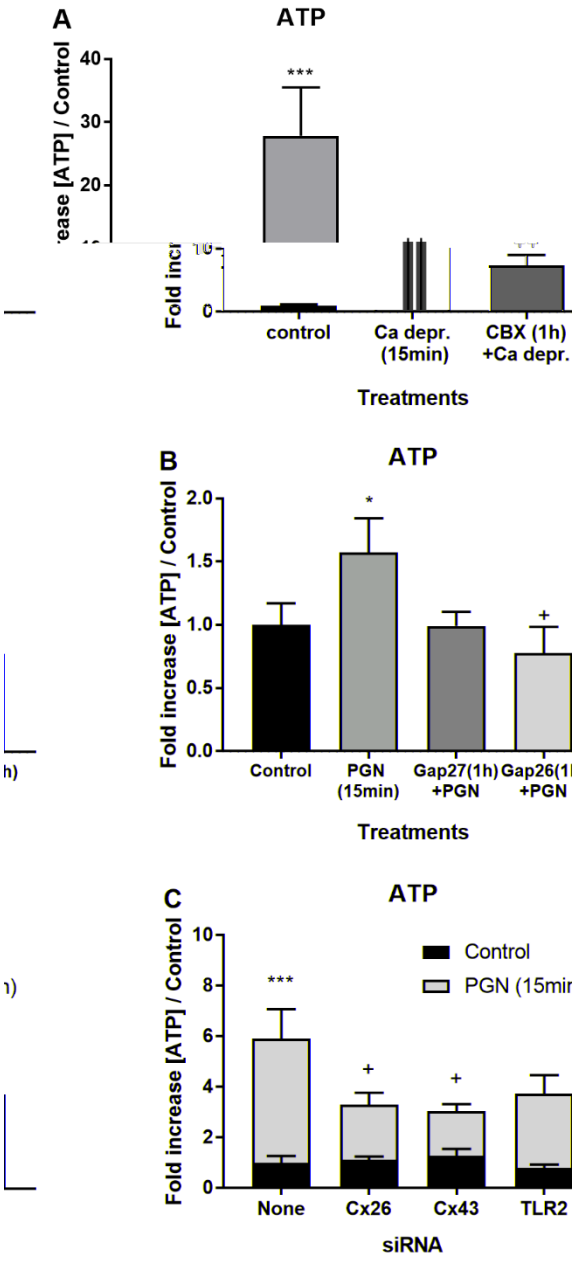

781

782 Figure 5

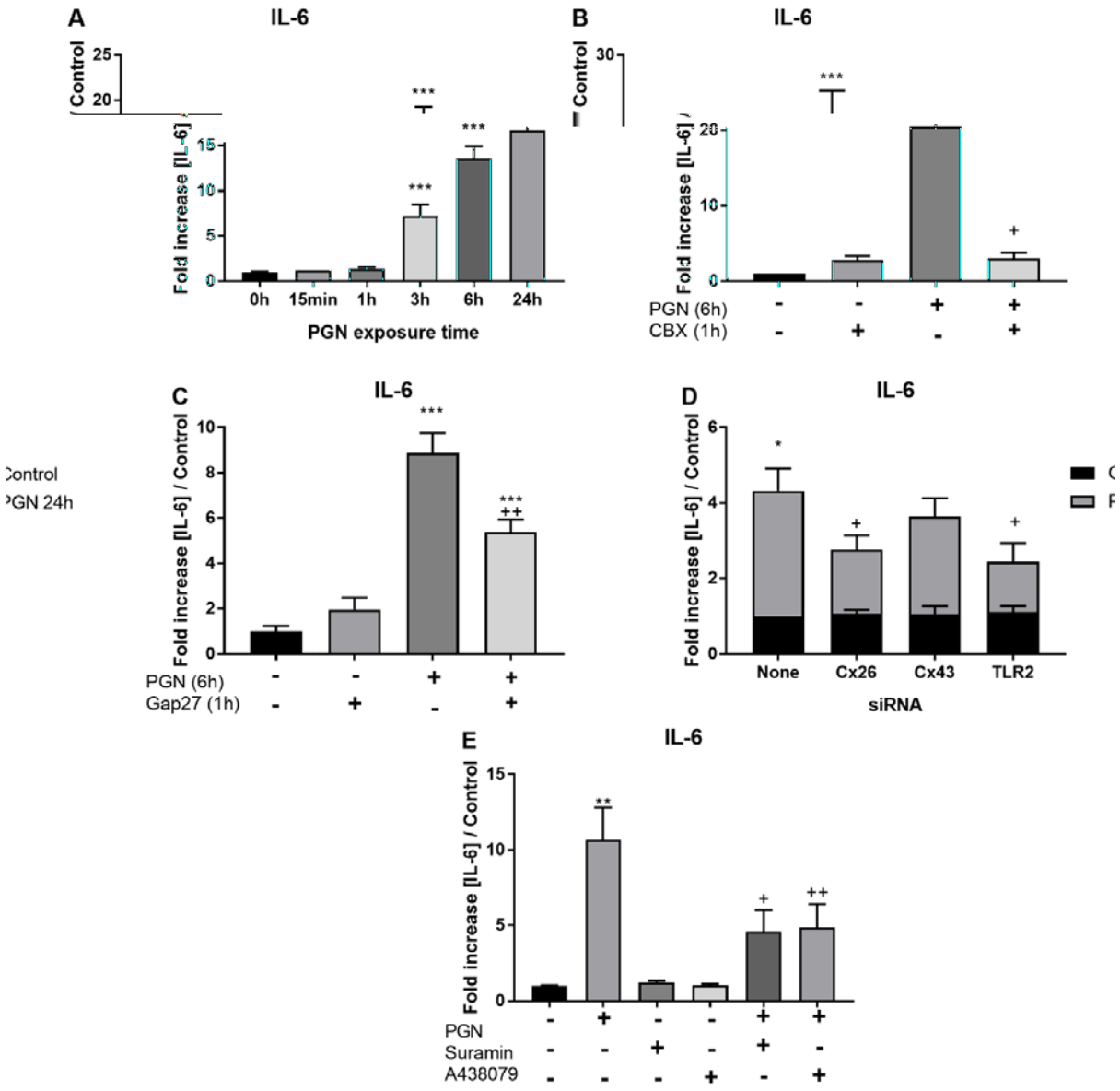

783

784

785 Figure 6

786

787

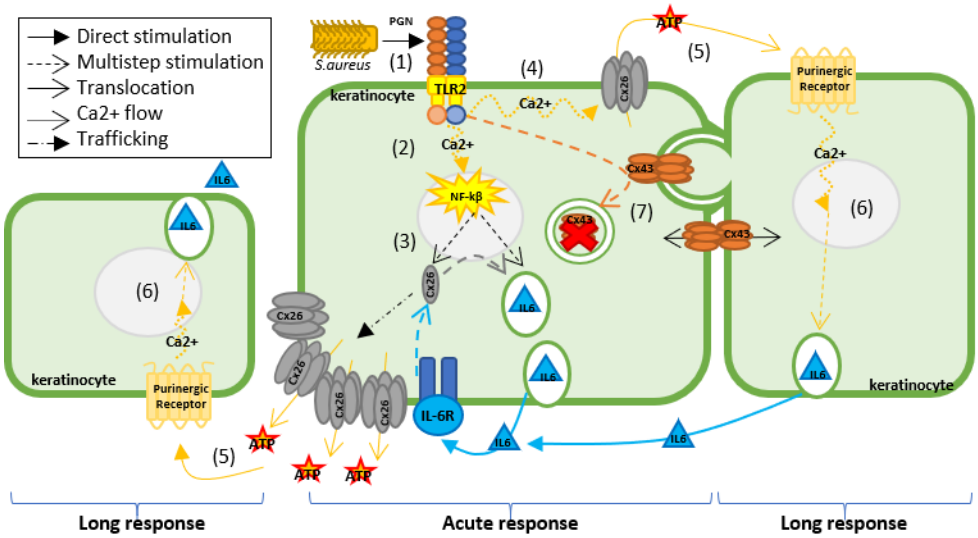

788

789 Figure 7

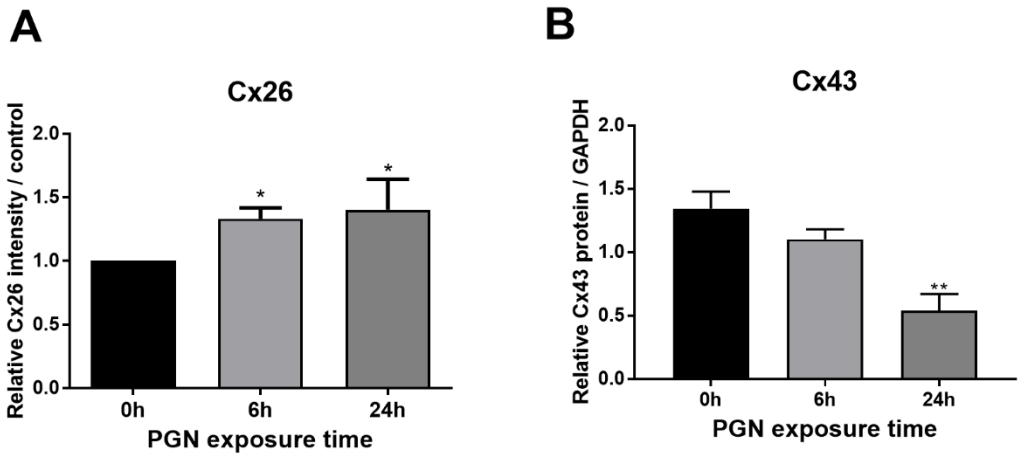

790

791 Suppl Fig 1

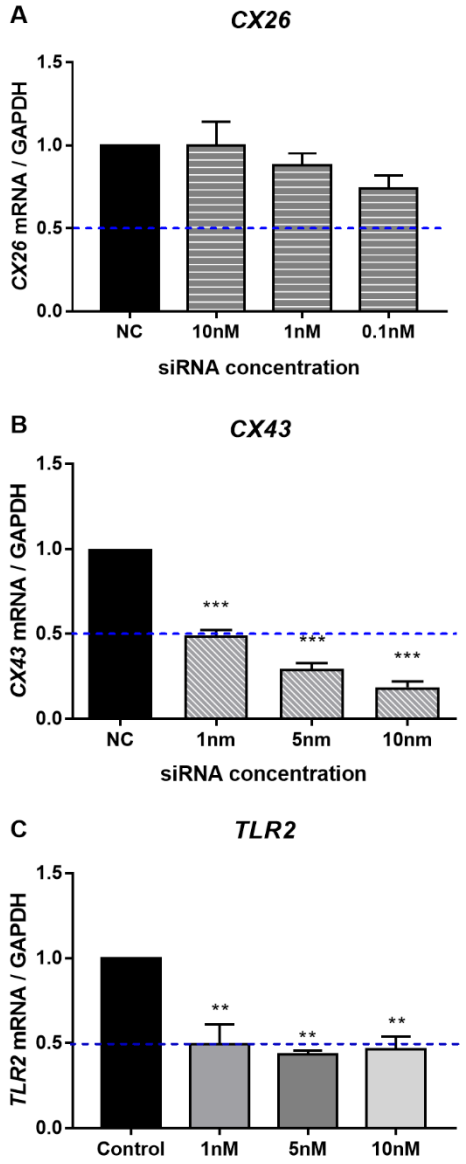

792

793 Supp Fig 2

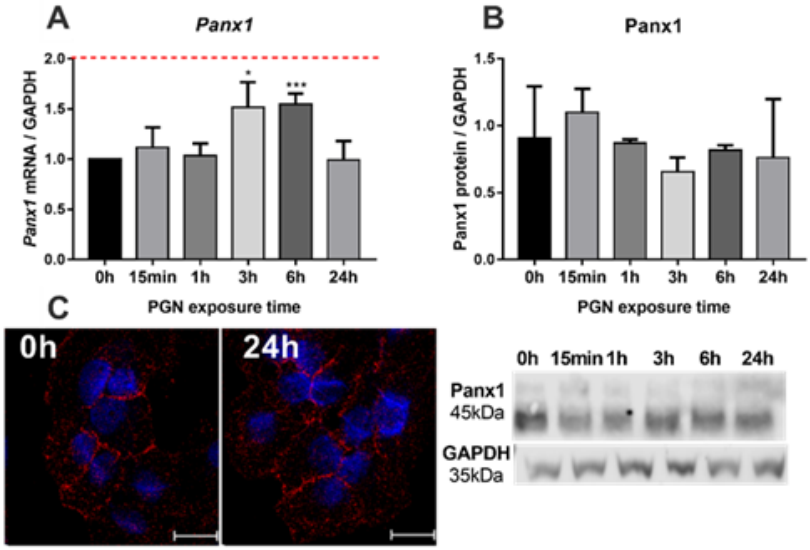

794

795 Supp Fig 3

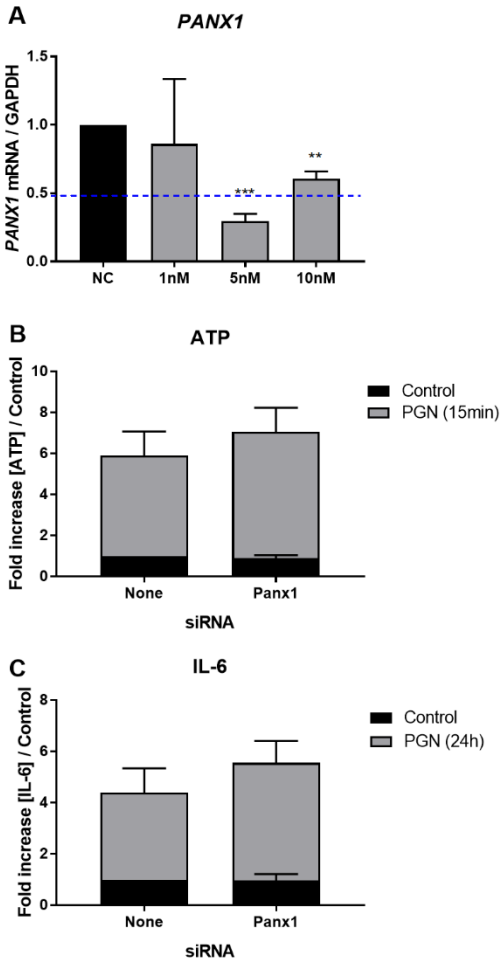

796

797 Supp Fig 4